This article has been accepted for publication in a future issue of this journal, but has not been fully edited. Content may change prior to final publication. Citation information: DOI 10.1109/JPHOT.2015.2507364, IEEE Photonics Journal

Visible light communication using receivers of camera image sensor and solar cell

Yang Liu[1], Hung-Yu Chen[2], Kevin Liang[2], Chin-Wei Hsu[2], Chi-Wai Chow[*,2], *Senior Member, IEEE*, and Chien-Hung Yeh[3]

[1]*Philips Electronics Ltd.*

[2]*Department of Photonics and Institute of Electro-Optical Engineering, National Chiao Tung University, Taiwan*

[3]*Department of Photonics, Feng Chia University, Seatwen, Taichung 40724, Taiwan*

**Corresponding author: cwchow@faculty.nctu.edu.tw*

Abstract: We propose an electronic label and sensor system using visible light communication (VLC). The downlink signal is transmitted by a white-light LED lamp which can provide lighting, VLC and energy harvesting for the mobile devices. The downlink is received by a solar cell. The uplink can be captured by the surveillance camera image sensor. However, using the camera image sensor as VLC receiver (Rx) is challenging since the data rate is limited by the frame rate; as well as uneven light exposure. Rolling shutter effect of the image sensor can be used to increase the data rate. In this work, we propose and demonstrate using a second order polynomial (SOP) extinction ratio (ER) enhancement scheme together with thresholding schemes of iterative and modified quick adaptive to demodulate the obtained rolling shutter pattern. The ER enhancement scheme can significantly reduce the large ER fluctuation. Experimental results show that by using the proposed SOP ER enhancement scheme, the bit-error rate (BER) improvement can be up to two orders of magnitude. We also believe that the proposed electronic label and sensor system may be applicable of internet-of-things (IoT) sensing networks for connecting a number of mobile devices.

Index Terms: Free space communication; Optical communications; Light emitting diode (LED)

1. Introduction

Wireless communication plays an important role in our daily lives, it is expected the future mobile data volume per area and number of connected devices will be 1,000 times and 100 times respectively higher than present wireless networks [1]. To provide such a high density and high capacity wireless communication is challenging, since the conventional RF spectrum has been congested, and the interference between nearby RF access points will be severe. Many literatures show that using visible light communication (VLC) based on light emitting diodes (LEDs) or lasers [2-8] can be a promising solution for future high density and high capacity wireless networks. VLC can provide an additional wireless communication channels using the visible spectrum; furthermore, as VLC is very directional, it can provide dedicated communication channel confining in a smaller area to reduce the interference. As a result, VLC is also regarded as one of the promising candidates for the fifth generation (5G) wireless networks [9]. Besides, Internet of Things (IoT) network is becoming more and more important, many devices can be connected for sensing, monitoring or resource sharing, and VLC could also play an important role.

Here we propose an electronic label and sensor system using VLC for optical wireless connection. The downlink signal is transmitted by a white-light LED lamp which can provide lighting, VLC and energy harvesting for the mobile devices. The downlink signal is received by a solar cell. In the mobile device, the environmental parameters are sent back to the control office (CO) as

This article has been accepted for publication in a future issue of this journal, but has not been fully edited. Content may change prior to final publication. Citation information: DOI 10.1109/JPHOT.2015.2507364, IEEE Photonics Journal

uplink signal, which can be captured by a surveillance camera image sensor. However, using the camera image sensor as VLC receiver (Rx) is challenging since the data rate is limited by the camera frame rate (~ 28 fps). Although a tailor-made complementary metal-oxide-semiconductor (CMOS) image sensor with specific high speed photo-diode (PD) for VLC and low speed pixels for imaging is proposed [10]; it can be costly. Rolling shutter effect of the CMOS camera is used to enhance the transmission data rate higher than the frame rate [11], and bright and dark fringes (rolling shutter pattern) can be obtained in each received frame. By demodulating these fringes, the data can be retrieved. However, [11] requires complicated histogram equalization together with Sobel edge detection for the bright and dark fringes extinction ratio (ER) enhancement.

In this work, we propose and demonstrate using a second order polynomial (SOP) ER enhancement scheme together with thresholding schemes of iterative and modified quick adaptive for the first time up to our knowledge to demodulate the rolling shutter pattern obtained in the CMOS image sensor. The ER enhancement scheme can significantly reduce the large ER fluctuation. Experimental results show that by using the proposed SOP ER enhancement scheme, the bit-error rate (BER) improvement can be up to two orders of magnitude.

2. Proposed Architecture

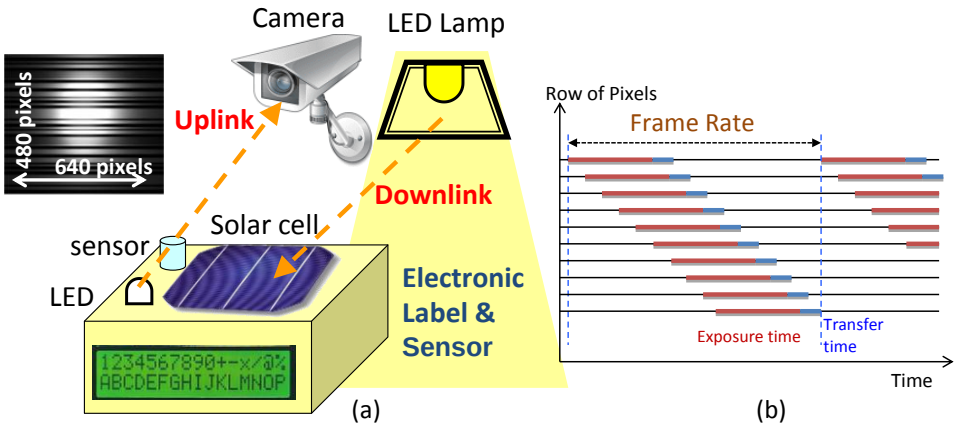

Fig. 1. (a) Proposed electronic label and sensor system using VLC for optical wireless connection, (b) mechanism of rolling shutter effect.

Fig. 1(a) shows our proposed electronic label and sensor system. The downlink signal is transmitted by a ceiling LED lamp which provides lighting, VLC and energy harvesting for the devices. The downlink signal is received by a solar cell panel. The mobile device can have different kinds of sensors, such as for temperature or humility sensing. The display in the mobile device can show the environmental parameters, or the price of commodities if used in department store. Then, the environmental parameters or monitoring information are sent back to the CO as uplink signal. This uplink signal can be captured by a surveillance camera image sensor. It is worth to point out that the proposed architecture can be a point to multiple points (multiple devices) system since the surveillance camera will scan over the entire area and receive uplink signals from many devices using time division multiple access (TDMA). Fig. 1(b) shows the mechanism of rolling shutter effect of the CMOS image sensor. During the image acquisition, each row of pixels is activated sequentially. Besides, there is a transfer time after the exposure time. This is the time required for combining different row of pixels into an image frame.

3. Experiment, Results & Discussion

A proof-of-concept experiment similar to Fig. 1(a) is performed. For the downlink, the pseudo-random data is generated in a computer Matlab program, which is then transferred to an arbitrary waveform generator (AWG, Tektronix, AFG 3252C) with 2 GSample/s sampling rate and 240 MHz bandwidth for digit-to-analog conversion (DAC). The AWG is used to drive a white-light LED (Cree

This article has been accepted for publication in a future issue of this journal, but has not been fully edited. Content may change prior to final publication. Citation information: DOI 10.1109/JPHOT.2015.2507364, IEEE Photonics Journal

XLamp XR-E). Then the white-light signal is received by a commercially available solar cell panel typically used in calculator. For the uplink, another AWG is used to drive a white-light LED in the mobile device. It is then received by a camera image sensor with 480 x 640 pixels resolution and 28 frame/second frame rate.

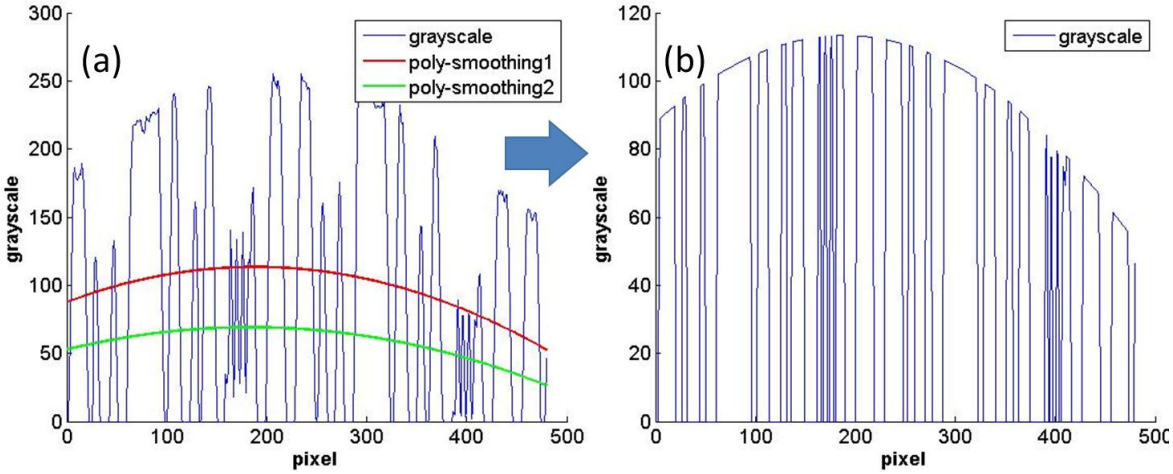

Fig. 2. Experimental grayscale values (a) before and (b) after applying the SOP ER enhancement.

We first discuss the uplink VLC signal captured by the camera image senor. The rolling shutter pattern (bright and dark fringes) can be observed in the inset of Fig. 1(a). The uplink VLC is packet-based, and each packet consists of a 4-bit header in Manchester coding and a 32-bit payload in on-off keying (OOK) format. A two minutes video is captured for each BER measurement to increase the BER reliability. In this proof-of-concept experiment, only a single moderate brightness white-light LED is used, and the transmission distance at ~ 500 lux is 26 cm. The transmission distance can be further enhanced by using higher brightness LEDs. The sensor cannot record any signal during the transfer time (Fig. 1(b)), and this time in our camera is 14.29 ms (~40% of an image frame). Hence, each data packet will be transmitted 3 times successively to ensure each image frame captured by the camera contains a complete data packet including both header and payload. Finally, the net data rate is ~1 kbit/s with deducting the duplicated data packets. Hence the uplink data rate can be increased from 28 bit/s to ~1 kbit/s. To demodulate the bright and dark fringes, the recorded video file is first converted into grayscale format (i.e. 255 represents complete brightness and 0 represents complete darkness). A vertical column of pixels (480 x 1) is selected [11] in each image frame to form a bit-pattern as shown in Fig. 2(a). A large ER fluctuation can be observed in Fig. 2(a). As the header is in Manchester coding format, much narrower fringes can be easily distinguished from the OOK payload data. Here, we propose and demonstrate a SOP ER enhancement scheme. The physical meaning of using SOP ER scheme is to construct a “smooth” mathematical equation that can approximately fit to a series of grayscale data values. In the first SOP curve fitting, the original grayscale values above the first SOP curve will be assigned equal to the SOP curve. After this, the second SOP curve fitting is constructed. Then, we set the interception points of the original grayscale curve and the second SOP curve to be zero. Hence the grayscale pattern will be more uniform. We now describe the mathematical algorithm. In the SOP ER enhancement scheme, the first SOP curve fitting is applied (red curve in Fig. 2(a)). Assume each element in the column matrix is (x_i, y_i), where x_i is the i^{th} pixel, and y_i is that pixel’s grayscale value. The SOP fitting curve $f(x_i)$ can be represented by Eq. (1),

$$f(x_i; a_0, a_1, a_2) = a_0 + a_1 x_i + a_2 x_i^2 \quad (1)$$

then the square deviation can be represented in Eq. (2),

$$[y_i - f(x_i)]^2 \quad (2)$$

and the total square deviation function E is represented in Eq. (3), we need to find the minimum value of this function.

This article has been accepted for publication in a future issue of this journal, but has not been fully edited. Content may change prior to final publication. Citation information: DOI 10.1109/JPHOT.2015.2507364, IEEE Photonics Journal

$$E(a_0, a_1, a_2) = \sum_{i=1}^{480} [y_i - f(x_i)]^2 = \sum_{i=1}^{480} [y_i - (a_0 + a_1 x_i + a_2 x_i^2)]^2 \quad (3)$$

By setting $\frac{\partial E}{\partial a_0}, \frac{\partial E}{\partial a_1}, \frac{\partial E}{\partial a_2} = 0$, we can obtain three simultaneous equations to solve for a_0, a_1, a_2. After obtaining a_0, a_1, a_2, the SOP fitting curve in Eq. (1) can be obtained. This is the first SOP curve (red curve in Fig. 2(a)). Then we set this curve to be the maximum grayscale value of each pixel. Next, the second SOP curve using similar algorithm as described in Eq. (1)-(3) is constructed (green curve in Fig. 2(a)). We set the interception points of the original grayscale curve and the green curve to be zero. As a result, the ER can be significantly enhanced, as shown in Fig. 2(b). The ER is defined as the ratio of grayscale value of high level to grayscale value of low level; hence the ER of the Manchester coded header (at ~ 160th pixel) increases from 6 to unlimited (since we force the grayscale value of low level to be 0). The ER fluctuations are also significantly.

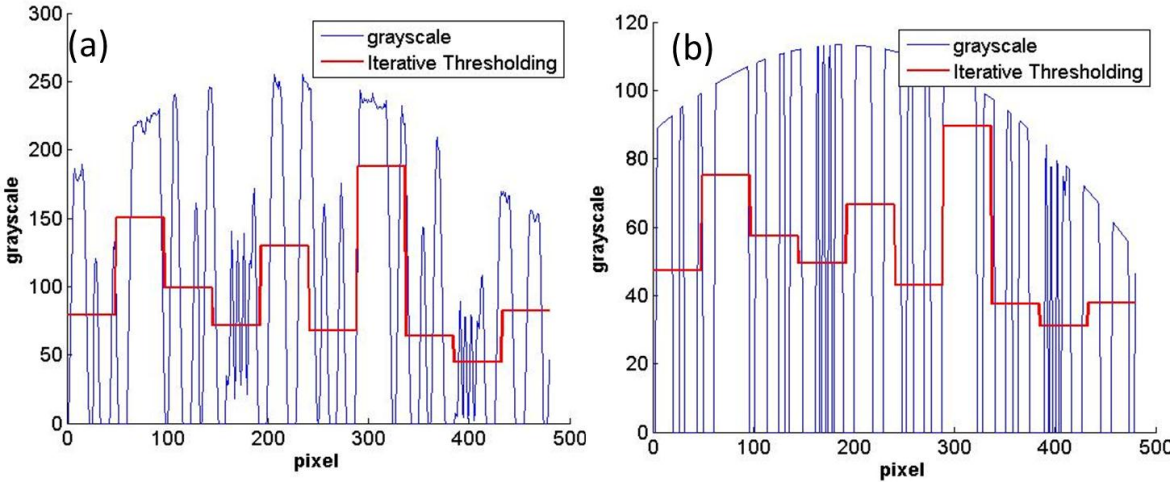

Fig. 3. Experimental grayscale values by applying the iterative thresholding scheme (a) without and (a) with using the SOP ER enhancement.

After the SOP ER enhancement, a thresholding scheme is needed to define the data logic; hence the grayscale value above the threshold is regarded as logic "1" while below the threshold is regarded as logic "0". A good thresholding scheme is to construct a mathematical equation in the middle of the grayscale pattern for defining the data logic. We first apply the iterative thresholding scheme [12], in which the whole data packet is divided into 10 sections; hence each section is consisted of 48 pixels. In our experimental analysis, dividing 10-section provides the optimum result. In each section, we apply iterative calculation. Assume y_i is the grayscale value of that pixel, i = 1, 2, … 48. The initial average grayscale value T in one section is shown in Eq. (4),

$$T = \sum_{i=1}^{48} \frac{y_i}{48} \quad (4)$$

hence two regions A_1 and A_2 depending on T can be obtained as shown in Eq. (5),

$$\begin{cases} y_i \in A_1, & y_i \geq T \\ y_i \in A_2, & y_i < T \end{cases} \quad (5)$$

the average grayscale values in regions A_1 and A_2 are calculated separately to obtain T_1 and T_2 respectively. The new threshold grayscale value T_k, can be expressed in Eq. (6).

$$T_k = \frac{T_1 + T_2}{2} \quad (6)$$

This article has been accepted for publication in a future issue of this journal, but has not been fully edited. Content may change prior to final publication. Citation information: DOI 10.1109/JPHOT.2015.2507364, IEEE Photonics Journal

The new T_k will replace the initial T in Eq. (4), and the process described above is repeated until $T_k = T$; hence the final threshold value can be obtained. Fig. 3(a) and (b) show the experimental grayscale values by applying the iterative thresholding scheme without and with using the SOP ER enhancement. We can roughly observe that using SOP ER enhancement can provide a better thresholding. The quantitative results will be provided later.

Secondly, we also applied our modified quick adaptive thresholding scheme, which is based on the adaptive thresholding [13]. Assume y_i be the grayscale value of a pixel at point i, and s is the number of pixels adjacent to point i, in this case, s = 60. The threshold value from our modified quick adaptive scheme can be expressed in Eq. (7),

$$\begin{cases} T_i = 0.8\dfrac{\sum_{n=0}^{s-1} y_{i-n}(1-\frac{1}{s})^n}{\sum_{n=0}^{s-1}(1-\frac{1}{s})^n}, & n \geq s \\ T_i = 0.8\dfrac{\sum_{n=0}^{s-1} y_{i+n}(1-\frac{1}{s})^n}{\sum_{n=0}^{s-1}(1-\frac{1}{s})^n}, & n < s \end{cases} \tag{7}$$

Fig. 4(a) and (b) show the experimental grayscale values by applying the quick adaptive thresholding without and with using the SOP ER enhancement. We can also roughly observe that using SOP ER enhancement can provide a better thresholding. The quantitative comparison results will be provided next paragraph.

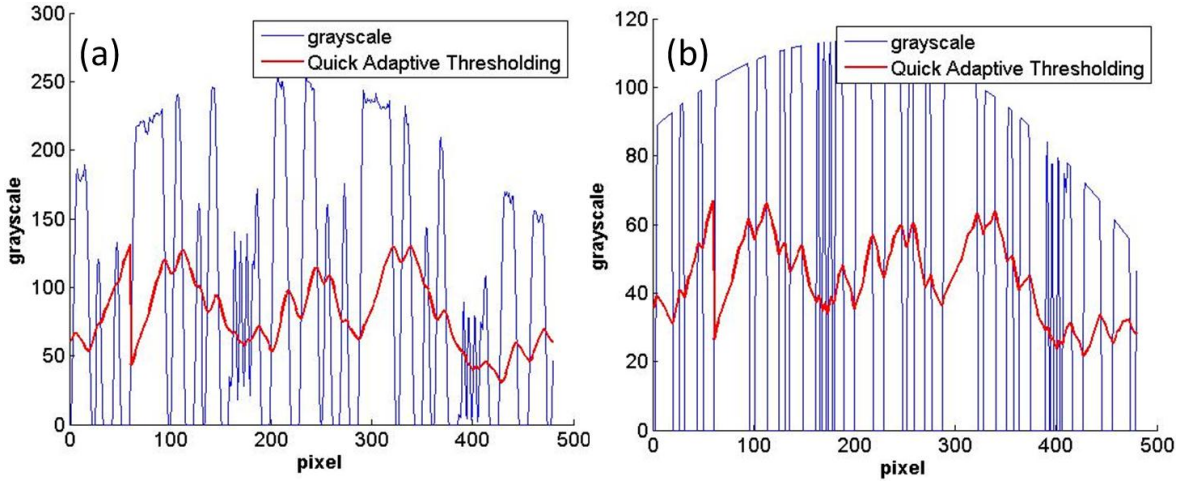

Fig. 4. Experimental grayscale values by applying the Quick adaptive thresholding (a) without and (b) with using the SOP ER enhancement.

Fig. 5(a) shows the BER performance of using iterative thresholding scheme without and with the SOP ER enhancement. The BER performance with the SOP ER enhancement can satisfy FEC at low illuminance (i.e. orange dotted line). Fig. 5(b) shows the BER of using modified quick adaptive thresholding scheme without and with using the SOP ER enhancement. As predicted before, using SOP ER enhancement shows a significant BER enhancement with up to 2 orders of magnitude.

This article has been accepted for publication in a future issue of this journal, but has not been fully edited. Content may change prior to final publication. Citation information: DOI 10.1109/JPHOT.2015.2507364, IEEE Photonics Journal

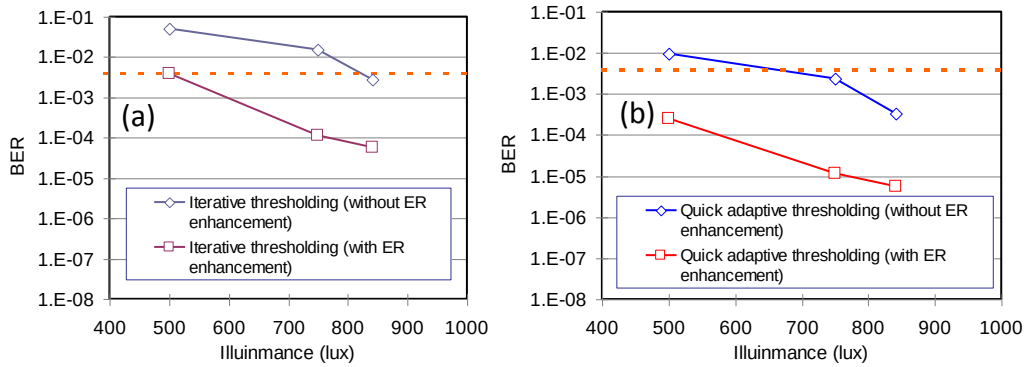

Fig. 5. Measured BER of (a) using iterative thresholding scheme and (b) quick adaptive thresholding scheme without and with using the SOP ER enhancement.

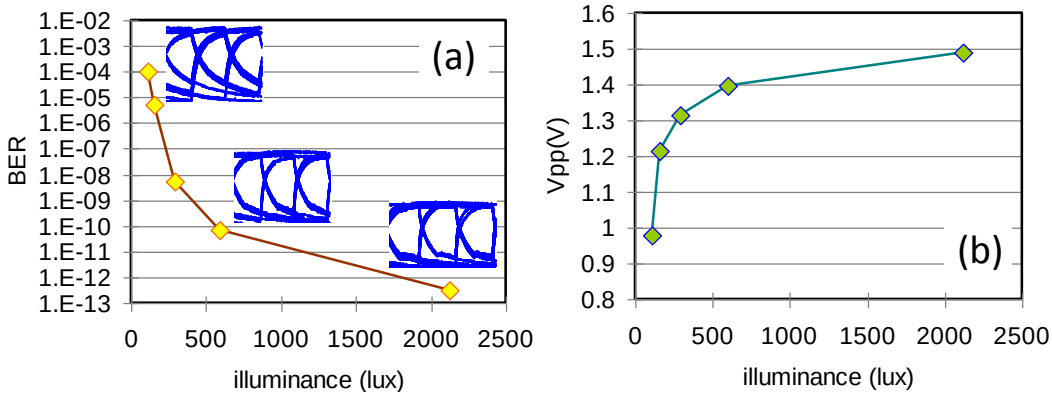

Fig. 6. (a) Measured BER at different illuminance and (b) the corresponding generated photo-voltage.

Finally, the BER of the downlink signal emitted by a white LED and received by a solar cell panel is performed. Fig. 6(a) shows the BER performance of the solar cell Rx at different illuminances with the corresponding eye-diagrams. In this demonstration, only 1 kbit/s is used; however, much higher data rates can be achieved by using the solar cell as the VLC Rx [14]. Due to the high capacitance effect of the solar cell, the rise and fall times of the received signal are limited. However, it is still good enough for detecting the downlink signal satisfying the FEC limit even at extremely low illuminance of 100 lux. The corresponding generated photo-voltage is shown in Fig. 6(b). As shown in Fig. 6(a), the relationship between BER and the illuminance is quite linear at low illuminance; when the illuminance is > 500 lux, the relationship becomes not linear. We believe that this may be due to the saturation of the solar cell at high illuminance; and we can also observe in Fig. 6(b) that the increase in V_{pp} is very small at high illuminance.

4. Conclusions

We proposed an electronic label and sensor system using VLC. Here, we also proposed and demonstrated a SOP ER enhancement scheme together with two thresholding schemes (iterative and modified quick adaptive schemes) for demodulation of the rolling shutter pattern. Experimental results showed that the SOP ER enhancement scheme can significantly enhance the BER performance; and the modified quick adaptive scheme outperformed the iterative scheme. On the other hand, BER of the downlink signal emitted by a white LED and received by a solar cell panel was performed. Experimental results show that the solar cell is good enough for detecting the downlink signal satisfying the FEC limit even at extremely low illuminance of 100 lux.

This article has been accepted for publication in a future issue of this journal, but has not been fully edited. Content may change prior to final publication. Citation information: DOI 10.1109/JPHOT.2015.2507364, IEEE Photonics Journal

Acknowledgement

This work was supported by Ministry of Science and Technology, Taiwan, ROC, MOST-104-2628-E-009-011-MY3, MOST-103-2221-E-009-030-MY3, Aim for the Top University Plan, Taiwan, and Ministry of Education, Taiwan.

References

[1] P. Pirinen, “A brief overview of 5G research activities,” Proc. Int. Conf. on 5G for Ubiquitous Connectivity 17-22 (2014).

[2] C. H. Chang, C. Y. Li, H. H. Lu, C. Y. Lin, J. H. Chen, Z. W. Wan, and C. J. Cheng, “A 100-Gb/s multiple-input multiple-output visible laser light communication system,” J. Lightw. Technol. 32, 4723-4729 (2014).

[3] B. Janjua, H. M. Oubei, J. R. Durán Retamal, T. K. Ng, C. T. Tsai, H. Y. Wang, Y. C. Chi, H. C. Kuo, G. R. Lin, J. H. He, and B. S. Ooi, “Going beyond 4 Gbps data rate by employing RGB laser diodes for visible light communication,” Opt. Express 23, 18746-18753 (2015).

[4] Y. C. Chi, D. H. Hsieh, C. T. Tsai, H. Y. Chen, H. C. Kuo, and G. R. Lin, "450-nm GaN laser diode enables high-speed visible light communication with 9-Gbps QAM-OFDM," Opt. Express 23, 13051-13059 (2015).

[5] W. Y. Lin, C. Y. Chen, H. H. Lu, C. H. Chang, Y. P. Lin, H. C. Lin, and H. W. Wu, "10m/500Mbps WDM visible light communication systems," Opt. Express 20, 9919-9924 (2012)

[6] C. W. Chow, C. H. Yeh, Y. Liu, and Y. F. Liu, “Digital signal processing for light emitting diode based visible light communication,” IEEE Photon. Soc. Newslett. 26, 9-13 (2012).

[7] H. H. Lu, Y. P. Lin, P. Y. Wu, C. Y. Chen, M. C. Chen, and T. W. Jhang, “A multiple-input-multiple-output visible light communication system based on VCSELs and spatial light modulators,” Opt. Express 22, 3468-3474 (2014).

[8] Z. Wang, C. Yu, W. D. Zhong, J. Chen, and W. Chen, “Performance of a novel LED lamp arrangement to reduce SNR fluctuation for multi-user visible light communication systems,” Opt. Express 20, 4564–4573 (2012).

[9] S. Wu, H. Wang, and C. H. Youn, “Visible light communications for 5G wireless networking systems: from fixed to mobile communications,” IEEE Network 28, 41-45 (2014).

[10] I. Takai, S. Ito, K. Yasutomi, K. Kagawa, M. Andoh, and S. Kawahito, “LED and CMOS image sensor based optical wireless communication system for automotive applications,” IEEE Photon. J. 5, 6801418 (2013).

[11] C. W. Chow, C. Y. Chen and S. H. Chen, “Enhancement of signal performance in LED visible light communications using mobile phone camera,” IEEE Photon. J. 7, 7903607 (2015).

[12] R. C. Gonzalez and R. E. Woods. Digital Image Processing. Pearson (2002).

[13] P. D. Wellner, “Adaptive thresholding for the digital desk,” Tech. Rep. EPC-93-110 (1993).

[14] Z. Wang, D. Tsonev, S. Videv, and H. Haas, “On the design of a solar-panel receiver for optical wireless communications with simultaneous energy harvesting,” IEEE J. on Sel. Areas in Comm. 33, 1612-1623 (2015).